Complex I-mediated reactive oxygen species generation: modulation by cytochrome *c* and NAD(P)$^+$ oxidation–reduction state

Yulia KUSHNAREVA, Anne N. MURPHY[1] and Alexander ANDREYEV
Mitochondrial Biology, MitoKor, 11494 Sorrento Valley Road, San Diego, CA 92024, U.S.A.

Several lines of evidence indicate that mitochondrial reactive oxygen species (ROS) generation is the major source of oxidative stress in the cell. It has been shown that ROS production accompanies cytochrome *c* release in different apoptotic paradigms, but the site(s) of ROS production remain obscure. In the current study, we demonstrate that loss of cytochrome *c* by mitochondria oxidizing NAD$^+$-linked substrates results in a dramatic increase of ROS production and respiratory inhibition. This increased ROS production can be mimicked by rotenone, a complex I inhibitor, as well as other chemical inhibitors of electron flow that act further downstream in the electron transport chain. The effects of cytochrome *c* depletion from mitoplasts on ROS production and respiration are reversible upon addition of exogenous cytochrome *c*. Thus in these models of mitochondrial injury, a primary site of ROS generation in both brain and heart mitochondria is proximal to the rotenone inhibitory site, rather than in complex III. ROS production at complex I is critically dependent upon a highly reduced state of the mitochondrial NAD(P)$^+$ pool and is achieved upon nearly complete inhibition of the respiratory chain. Redox clamp experiments using the acetoacetate/D-β-hydroxybutyrate couple in the presence of a maximally inhibitory rotenone concentration suggest that the site is approx. 50 mV more electronegative than the NADH/NAD$^+$ couple. In the absence of inhibitors, this highly reduced state of mitochondria can be induced by reverse electron flow from succinate to NAD$^+$, accounting for profound ROS production in the presence of succinate. These results lead us to propose a model of thermodynamic control of mitochondrial ROS production which suggests that the ROS-generating site of complex I is the Fe–S centre N-1a.

Key words: brain, electron transport chain, heart, mitochondria, superoxide.

INTRODUCTION

In multiple apoptotic paradigms, oxidative stress accompanies activation of the mitochondria-linked death signal cascade that includes cytochrome *c* release as a commitment step (e.g. see [1–3] for review). The causative link between cytochrome *c* release and reactive oxygen species (ROS) production is still debated owing in part to a limited understanding of the mechanisms of mitochondrial ROS production. Due to the documented antioxidant functions of cytochrome *c* [4,5], one might propose that increased cellular ROS production during apoptosis results from the loss of the antioxidant function of cytochrome *c* at the mitochondria. Alternatively, loss of cytochrome *c* from mitochondria results in reversible inhibition of respiration [6] that may potentiate ROS production through reduction of a proximal site in the electron transport chain (e.g. [2]). In fact, stimulation of ROS production accompanying cytochrome *c* release and inhibition of mitochondrial respiration has been shown in apoptotic [7] and excitotoxicity [8] models. However, there are data to the contrary that depletion of isolated mitochondria of cytochrome *c* strongly inhibits H_2O_2 production. In this instance, the mitochondria were oxidizing succinate and were exposed to antimycin A [9].

With regard to mechanistic aspects of mitochondrial ROS generation, the studies following pioneering work by Boveris and Chance [10] pin-pointed auto-oxidation of the ubisemiquinone radical of coenzyme Q located in the o-centre of complex III as the mechanism of superoxide generation in mitochondria oxidizing succinate and treated with antimycin A [9,11,12]. In this instance, ubiquinol is oxidized in a sequential two-step electron transfer reaction with the first electron donated to the iron–sulphur Rieske protein and the second one to cytochrome *b* of complex III (see [13] for a review). Antimycin A indirectly prevents the second step, resulting in accumulation of ubisemiquinone, and hence increases ROS generation [10,14]. Inhibitors blocking the first step either directly (myxothiazol, stigmatellin) or indirectly through downstream inhibition of electron flow (complex IV inhibitors or cytochrome *c* depletion) prevent ROS production at this site [9,12,15]. In the latter case, this inhibition is due to reduction of the Fe–S cluster in the Rieske protein and therefore to inhibition of ubisemiquinone formation.

A second source of ROS production in the electron transport chain has been attributed to complex I [15] but the precise nature of the site and its contribution to mitochondrial ROS production remain obscure. A puzzling observation reported in several studies of mitochondria from different tissues is that, in the absence of antimycin A, ROS production in the presence of NAD$^+$-linked substrates is barely detectable, whereas succinate-supported respiration results in high rates of H_2O_2 production (e.g. [16,17]). The latter mechanism involves reverse electron flow from succinate to NAD$^+$, providing reducing equivalents to a redox carrier of complex I that serves as a site of ROS production (e.g. [16–20]). The process is inhibited by rotenone, blocking electron flow between the ubiquinone and the iron–sulphur centre

Abbreviations used: FCCP, *p*-trifluoromethoxyphenylhydrazone carbonyl cyanide; β-HOB, D-β-hydroxybutyrate; ROS, reactive oxygen species; *ROS site, site of superoxide generation.

[1] To whom correspondence should be addressed (e-mail murphya@mitokor.com).

N-2 [15,17,19,21–23]. Given the fact that the primary source of reducing equivalents to the mitochondrial respiratory chain is NADH rather than $FADH_2$, the relevance of succinate-supported ROS production remains unclear.

The objective of the present study was to explore the mechanistic link between cytochrome *c* release and ROS generation by using intact isolated heart and brain mitochondria energized with physiologically relevant NAD^+-linked respiratory substrates as a source of reducing equivalents. Here we show that extraction of cytochrome *c* significantly stimulates ROS production in mitochondria in the presence of glutamate and malate. To identify the site of ROS production, a comparison with the effects of specific inhibitors of mitochondrial respiration was performed and corresponding NADH levels were measured. In addition, an oxidation/reduction clamp was used to estimate the redox potential of the site. Some of these results have been presented in abstract form [24].

MATERIALS AND METHODS

Preparation of mitochondria

Brain mitochondria were isolated by differential centrifugation from rat forebrains using the method of Rosenthal et al. [25] with minor modifications [26]. This method, which employs digitonin to disrupt synaptosomes, yields a preparation of brain mitochondria including both synaptosomal and non-synaptosomal fractions. Heart mitochondria (a mixture of interfibrillar and subsarcolemmal organelles) were isolated by differential centrifugation according to published protocols [27], with the following modifications. The isolation buffer contained 250 mM mannitol, 70 mM sucrose, 5 mM Hepes/KOH, pH 7.4, 1 mM EGTA and 0.1 % BSA (fatty acid free). The mitochondrial pellet was washed once and resuspended in the isolation buffer without EGTA. The protein contents in the mitochondrial suspensions were 20–30 and 30–40 mg/ml for brain and heart respectively.

Cytochrome *c*-depleted mitochondria were prepared using the osmotic shock/high-salt extraction procedure as described by Turrens and co-workers [9].

Incubation conditions

For measurements of ROS generation, NADH, and oxygen consumption, mitochondria were incubated at 0.25 or 0.4 mg/ml (as indicated in the Figure legends) at 25 °C in a basal incubation medium containing 250 mM sucrose, 10 mM Hepes/KOH, pH 7.4, 25 μM EGTA and 2 mM phosphate, supplemented with either a mixture of 5 mM glutamate and 5 mM malate or with 5 mM succinate alone as respiratory substrates.

Oxygen consumption and NADH measurements

Oxygen consumption was measured using a Clark-type oxygen electrode (Diamond General) and an oxygen meter (Yellow Spring Instruments). NAD(P)H was measured by fluorescence at 340/460 nm in an LS50B spectrofluorometer (Perkin Elmer) and calibrated using 0.5 μM *p*-trifluoromethoxyphenylhydrazone carbonyl cyanide (FCCP) to induce a maximally oxidized state [0 % NAD(P)H] and 2 μM rotenone to induce a maximally reduced state [100 % NAD(P)H].

Detection of H_2O_2

The recently developed Amplex Red assay (Molecular Probes) for H_2O_2 detection is based on the enzymic reduction of H_2O_2 by horseradish peroxidase coupled with oxidation of the fluorogenic indicator Amplex Red. Typical measurements of mitochondrial generation of H_2O_2, followed by an exogenous pulse of H_2O_2, demonstrated that the horseradish peroxidase-based detection system responded almost instantly to addition of exogenous H_2O_2, outpacing the relatively low rates of mitochondrial ROS production (results not shown). It is noteworthy that no spontaneous oxidation of Amplex Red by mitochondria in the absence of horseradish peroxidase was observed within the time frame of experimental runs. Thus the detection system appears to be suitable for quantification of H_2O_2 production. The concentrations of horseradish peroxidase and Amplex Red in the basal incubation medium were 0.8 units/ml and 20 μM respectively. Fluorescence was recorded in an LS50B spectrofluorimeter or in a Polarstar plate reader (BMG) using 560 nm excitation and 590 nm emission wavelengths.

Redox titration

For the redox titration experiments, 0.8 mg of mitochondria were preincubated in 1.5 ml of the basal incubation medium without respiratory substrates for 10 min at 25 °C. At the end of this time period, 2 μM rotenone was added, followed by additions of 0.5 ml of the medium containing D-β-hydroxybutyrate (β-HOB, 99 % purity; Aldrich) to attain a final composition of 187.5 mM sucrose, 35 mM β-HOB, 20 mM Hepes/KOH, pH 7.4, 25 μM EGTA, 2 mM phosphate, the H_2O_2 detection system (see above) and various concentrations of acetoacetate to establish appropriate redox states of mitochondrial NAD(P)H. The samples were transferred into a 96-well plate, and the reaction rates were monitored in the Polarstar plate reader for 10 min.

Western blot for cytochrome *c*

The amount of cytochrome *c* in mitochondria was assessed by Western blot. Aliquots of samples from respiration experiments were run on 4–12 % Mes NuPage gels (Novex) for 42 min at 200 V and 4 °C. The subsequent wet electrotransfer to nitrocellulose membrane was performed using a Novex system with 5 % methanol in the transfer buffer for 1 h at 30 V. The transfer efficiency was confirmed by post-transfer staining of the gel and the membrane with EasyStain (Novex) and Ponceau S respectively. The membrane, washed of the residual stain with Tris-buffered saline with 0.2 % Tween-20 (TBS-T), was blocked overnight with 1.5 % dried milk in TBS-T. Cytochrome *c* was immunostained using primary mouse cytochrome *c* antibody (Pharmingen) at a 1:2000 dilution in TBS-T with 1.5 % milk for 1 h. Following incubation with secondary anti-mouse Ig linked to horseradish peroxidase (Amersham) at a 1:2000 dilution for 40 min, the band was visualized using luminol reagent and X-ray film.

Reagents

Reagents were from Sigma unless indicated otherwise.

RESULTS

Cytochrome *c* release causes ROS production in a site proximal to the rotenone inhibitory site in complex I

The high sensitivity of the Amplex Red assay permitted detection of low rates of ROS production by mitochondria oxidizing glutamate and malate (Figure 1A and Table 1). As expected, rates of succinate-supported ROS production were dramatically higher (Figure 1A and Table 1). As shown in Figure 1(A), cytochrome *c* depletion significantly stimulated ROS production

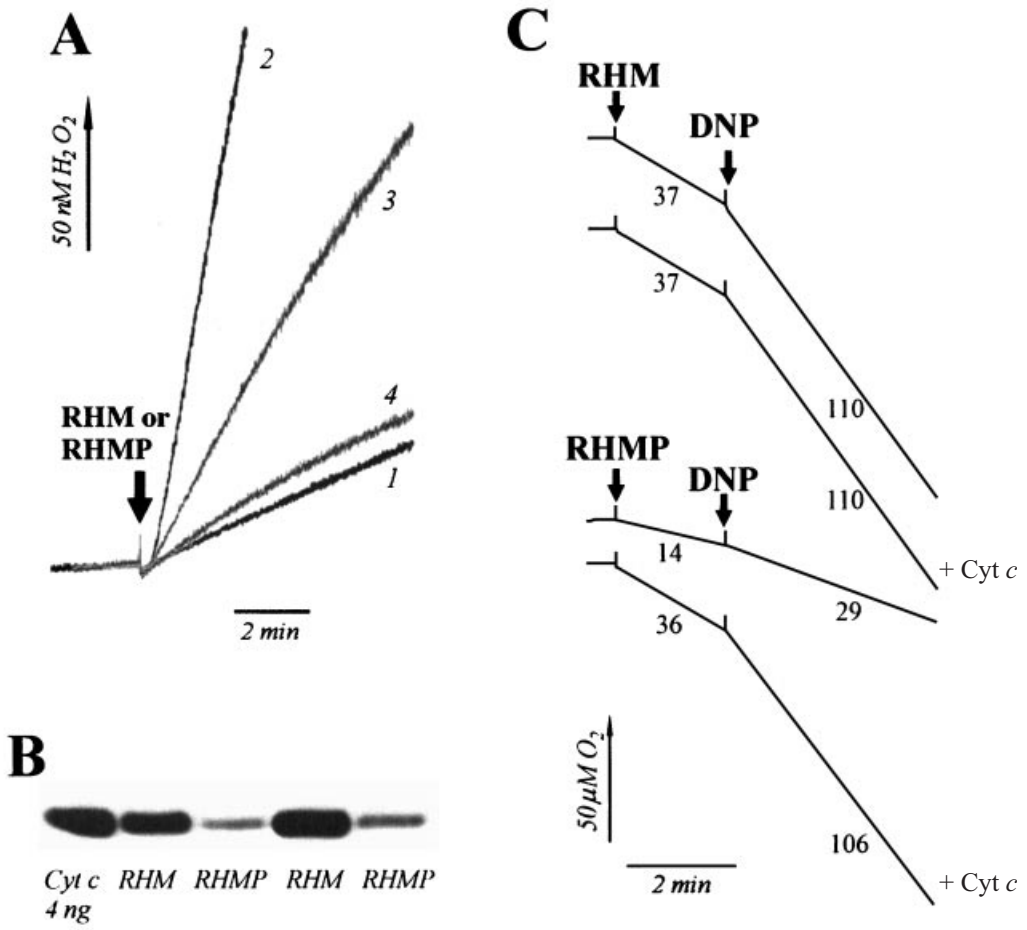

Figure 1 ROS production (A), cytochrome *c* content (B) and oxygen consumption (C) measured in rat heart mitochondria depleted of cytochrome *c* by osmotic shock/high-salt extraction

At the arrows, control mitochondria (RHM, 0.25 mg/ml), cytochrome *c*-depleted mitochondria (mitoplasts, RHMP, 0.25 mg/ml) and 2,4-dinitrophenol (DNP, 60 μM) were added. Data shown are from a representative experiment. (**A**) RHM and RHMP were incubated as described in the Materials and methods section. Traces 1 and 2, RHM oxidizing glutamate + malate (trace 1) or succinate (trace 2); traces 3 and 4, RHMP oxidizing glutamate and malate in the absence (trace 3) or presence (trace 4) of added cytochrome *c* (Cyt *c*, 6 μM). (**B**) Cytochrome *c* was measured by Western blot as described in the Materials and methods section. Samples were taken in the same experiment shown in (**A**) and (**C**), and from a separate mitochondrial preparation. (**C**) Oxygen consumption was measured in RHM and RHMP oxidizing succinate either in metabolic State 4 or in the presence of 2,4-dinitrophenol (uncoupled respiration). When present, cytochrome *c* concentration was 6 μM. Oxygen consumption data are given in nmol · min^{-1} · mg of $protein^{-1}$. Other details were as specified in the Materials and methods section.

Table 1 H_2O_2 production in control and cytochrome *c*-depleted mitochondria oxidizing different respiratory substrates

Effect of added cytochrome *c*. Results are means ± S.E.M. Values in parentheses are the number of separate mitochondrial preparations. Experimental conditions were as specified in the Materials and methods section.

	Rate of H_2O_2 production (pmol/min per mg of protein)	
Substrate	Heart	Brain
Glutamate/malate		
Control mitochondria	27 ± 2 (8)	29 ± 6 (4)
Cytochrome *c*-depleted mitochondria	86 ± 8 (8)	92 ± 18 (4)
Cytochrome *c*-depleted mitochondria + cytochrome *c*	31 ± 4 (6)	54 ± 15 (3)
Succinate		
Control mitochondria	294 ± 20 (8)	264 ± 14 (4)
Cytochrome *c*-depleted mitochondria	144 ± 31 (7)	231 ± 45 (4)

in mitochondria in the presence of glutamate and malate, and this effect was reversed upon the addition of exogenous cytochrome *c*. Western blot data confirmed that mitochondria that had undergone the osmotic shock/high-salt extraction procedure lost a significant portion of the total pool of cytochrome *c* (Figure 1B). This treatment resulted in partial and reversible inhibition of respiration (Figure 1C). It should be noted, however, that the extent of inhibition of respiration by cytochrome *c* depletion and, accordingly, the enhancing effects on ROS production, were variable between mitochondrial preparations (Table 1). Interestingly, cytochrome *c* depletion stimulated ROS in mitochondria oxidizing glutamate plus malate, but not in those oxidizing succinate. In fact, inhibition of respiration by cytochrome *c* depletion decreased succinate-supported ROS generation (Table 1). The latter observation is consistent with the requirement of a high membrane potential for succinate-supported ROS production in the absence of antimycin A (e.g. [10,16–18,28–30]). Exogenous cytochrome *c* did not inhibit ROS

Table 2 Effect of inhibitors of mitochondrial respiration on H_2O_2 production by mitochondria oxidizing glutamate and malate

Results are means ± S.E.M. Values in parentheses are the number of separate mitochondrial preparations. Experimental conditions were as specified in the Materials and methods section. MPP^+, 1-methyl-4-phenylpyridinium.

	Rate of H_2O_2 production (pmol/min per mg of protein)	
Inhibitor	Heart	Brain
None	30 ± 5 (6)	35 ± 6 (4)
Rotenone (2 μM)	201 ± 29 (6)	372 ± 39 (4)
Myxothiazol (1 μM)	138 ± 23 (6)	222 ± 8 (4)
Stigmatellin (2 μM)	123 ± 13 (6)	215 ± 19 (4)
MPP^+ (2 mM)	270 ± 46 (5)	448 ± 56 (4)

production in cytochrome *c*-depleted mitochondria oxidizing succinate (results not shown). Thus the observed changes in ROS generation caused by cytochrome *c* release are related to cytochrome *c*-linked electron transport rather than to direct radical-scavenging activity of cytochrome *c*. As shown in Table 1, cytochrome *c* depletion produces similar changes in ROS production in both heart and brain mitochondria.

The effect of cytochrome *c* release can be mimicked qualitatively by different site-specific inhibitors of the respiratory chain (Table 2). In agreement with previous observations, ROS production was stimulated in the presence of NAD^+-linked substrates and either rotenone [15,17,20,31,32] or MPP^+ (1-methyl-4-phenylpyridinium) [33], both of which are complex I inhibitors. Furthermore, myxothiazol and stigmatellin, the inhibitors that likewise inhibit ROS production in complex III, also stimulated H_2O_2 generation in the presence of glutamate and malate. Again, no qualitative differences between heart and brain mitochondria were observed in these models.

The absolute rates of ROS production in cytochrome *c*-depleted mitochondria (Table 1) are lower then those observed with respiratory inhibitors (Table 2). This difference is consistent with retention of a minor fraction of cytochrome *c* (Figure 1B) and therefore measurable, although decreased, respiratory activity (Figure 1C). In contrast, the concentrations of the inhibitors that were used caused complete respiratory inhibition.

Taken together, these data suggest that there is a common mechanism leading to ROS production in response to cytochrome *c* release and to the addition of inhibitors that block electron flow in different segments of the respiratory chain. Since downstream inhibition of electron flow leads to reduction of all upstream carriers because of mass action, this common mechanism appears to be the reduction of a carrier upstream of the most proximal inhibitory site (the rotenone-binding site). The current literature accepts that this site is located in complex I of the respiratory chain (e.g. [15–17,23,32,34–36]).

Near-maximal reduction of mitochondrial $NAD(P)^+$ is required for active ROS production

To assess the status of the proximal redox components we measured NAD(P)H levels. In a representative experiment shown in Figure 2(A), the NAD(P)H level in energized cytochrome *c*-depleted mitochondria oxidizing glutamate and malate is higher than in control mitochondria, a result that is consistent with significant inhibition of respiration as shown in Figure 1. As expected, additions of FCCP and rotenone to cytochrome

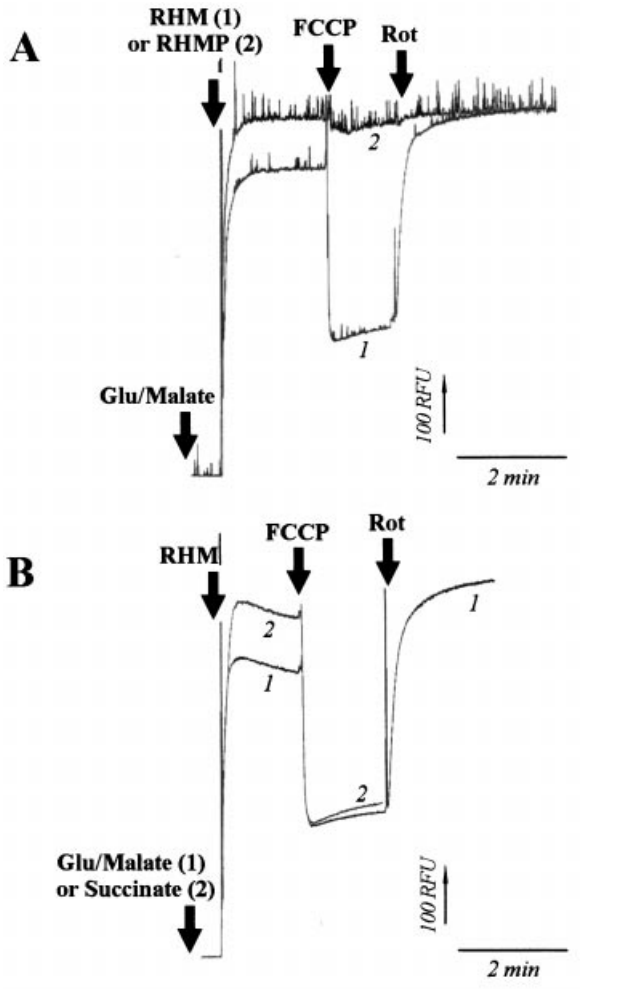

Figure 2 Changes in NAD(P)H levels after cytochrome *c* depletion (A) and in the presence of different respiratory substrates (B)

(**A**) Trace 1, control heart mitochondria (RHM, 0.4 mg/ml); trace 2, cytochrome *c*-depleted heart mitochondria (RHMP, 0.25 mg/ml). (**B**) Trace 1, glutamate and malate; trace 2, succinate. Other details were as specified in the Materials and methods section. Rot, rotenone.

c-depleted mitochondria caused minimal changes in the NAD(P)H level. These data, combined with those of Figure 1 and Table 1, indicate that near-maximal reduction of $NAD(P)^+$ in cytochrome *c*-depleted mitochondria is associated with increased ROS production, whereas the moderately lower levels of NAD(P)H in control mitochondria correspond to very low rates of ROS production. A similar enhancement of NAD(P)H levels was observed in the presence of succinate versus NAD^+-linked substrates (Figure 2B). We suggest that this enhanced level of reduction of pyridine nucleotides accounts for the higher rates of ROS production supported by reverse electron transport from succinate when compared with conditions of forward electron flow in the presence of NAD^+-linked substrates (Table 1).

As noted above, stimulation of ROS production in cytochrome *c*-depleted mitochondria was generally lower than in the presence of respiratory inhibitors and was variable between preparations owing to the variable residual cytochrome *c* (Figure 1B). Therefore, the use of respiratory inhibitors represented a more quantitatively consistent approach to study the mechanism of ROS production. Among those inhibitors, we have chosen rotenone

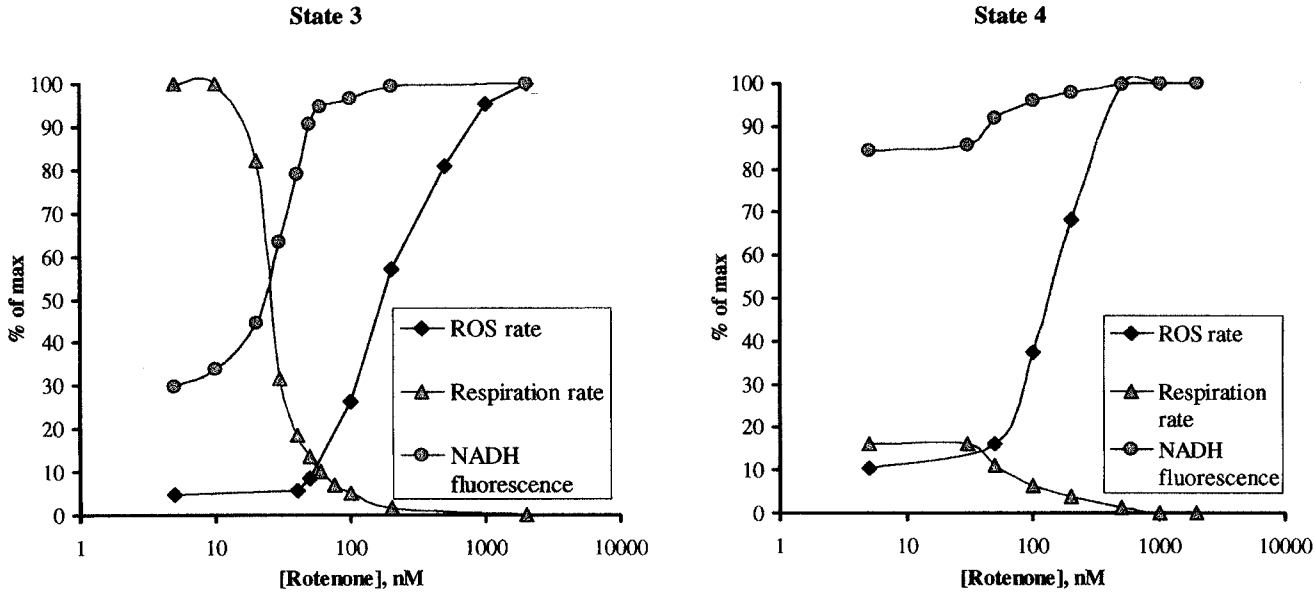

Figure 3 Dose-dependence of rotenone-induced ROS production, respiratory inhibition and NAD(P)$^+$ reduction in heart mitochondria in metabolic State 3 (left-hand panel) and State 4 (right-hand panel)

To induce State 3, mitochondria were incubated in the presence of 200 μM ADP, 1 mM $MgCl_2$, 10 mM glucose and 2 units/ml hexokinase. Concentration of mitochondrial protein was 0.4 mg/ml. ROS generation is expressed as a percentage of the rate in the presence of 2 μM rotenone, respiration as a percentage of the maximal rate in metabolic State 3, and NAD(P)H levels as a percentage of the maximal fluorescence. Other details were as specified in the Materials and methods section.

because it offered the additional advantage of being clinically relevant to Parkinson's disease [37].

ROS production in a site proximal to the rotenone inhibitory site

In agreement with earlier studies with submitochondrial membrane preparations [34,38], our data [24] and the data of others [39] on intact mitochondria indicated that near-complete respiratory inhibition by rotenone was required to detect even slightly increased ROS production. To address this paradox, we measured the redox status of upstream electron carriers relative to NAD(P)H levels. The data of Figure 3 show the similarity in the rotenone dose-responses of rates of ROS production in mitochondria that are either in metabolic State 3 (ADP-stimulated respiration) or 4 (resting respiration). Although in the absence of rotenone the NAD(P)H levels in the two metabolic states are dramatically different, note that the rates of ROS production are similarly low. In both states, stimulation of ROS generation begins only when rotenone increases the degree of NAD(P)$^+$ reduction to nearly maximal levels, and that these levels correspond to almost complete respiratory inhibition. This, in fact, may also be the mechanism underlying the significant difference in rates of glutamate/malate-supported ROS production in response to respiratory inhibitors versus that in response to cytochrome *c* depletion (Table 1).

Thus the rate of ROS production appears to be regulated by the NAD(P)H level, but this regulation begins only as pyridine nucleotides reach approx. 85 % of the maximally reduced level. In slightly less reduced states (e.g. with the lowest concentrations of rotenone in state 4), the rate of ROS generation is low and largely independent of NAD(P)H level. These data could indicate that ROS production is controlled by the NAD(P)H/NAD(P)$^+$ ratio, rather than simply the NAD(P)H level. Thus the ROS-generating site may be a highly negative redox centre under thermodynamic rather than kinetic control from component(s) of mitochondrial oxidative metabolism upstream of the rotenone-binding site in complex I (see the Discussion). To further characterize the putative ROS-generating site, we attempted determination of its midpoint potential using a redox titration approach.

Redox titration of ROS generation

The mitochondrial inner membrane prevents direct manipulation with the state of pyridine nucleotides. Therefore the β-HOB/acetoacetate redox couple was used to poise NAD(P)$^+$/NAD(P)H. Preliminary experiments demonstrated that rat heart mitochondria started to swell and lose respiratory control at levels of β-HOB in excess of approx. 25 % of total osmolarity (results not shown). Therefore, the substrate concentration was restricted to the maximal tolerable level of 35 mM.

Mitochondria from different tissues are capable of the reversible oxidation of β-HOB by NAD$^+$ (eqn 1). Although activity of the specific dehydrogenase in heart mitochondria is approx. 10 % of its activity in liver mitochondria [40], our experiments with rotenone-treated mitochondria show that the steady-state levels of NAD(P)H were established within approx. 10–15 min after addition of the redox couple (results not shown). This result indicates that the equilibrium can be reached within the normal time frame of our experiment and that the couple is appropriate for redox titration.

$$\beta\text{-HOB} + \text{NAD}^+ \leftrightarrow \text{acetoacetate} + \text{NADH} + \text{H}^+$$
$$K_{eq}^{7.0} = 0.0493,\ E_{1/2}^{(\beta\text{-HOB/acetoacetate})} = -281\ \text{mV} \quad (1)$$

Data in the literature on the redox properties of the β-HOB/acetoacetate couple are variable. We first undertook to estimate the apparent equilibrium constant (K_{eq}) and midpoint potential ($E_{1/2}$) for the couple in intact mitochondria by measuring NAD(P)H levels at different redox potentials of this couple. Our

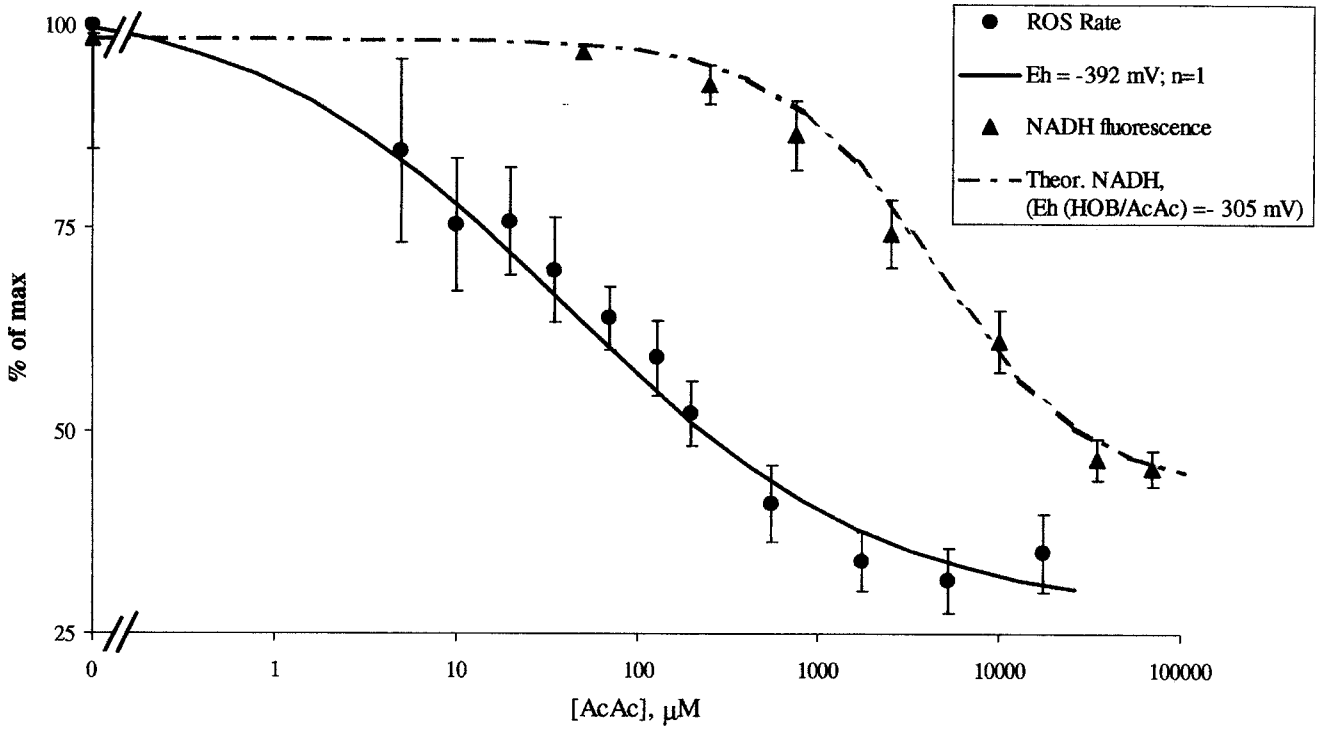

Figure 4 Redox titration of the proximal site of ROS production in rotenone-treated mitochondria

ROS generation was expressed as a percentage of the rate in the presence of β-HOB alone and NAD(P)H levels were expressed as a percentage of maximal fluorescence. The concentration of mitochondrial protein was 0.4 mg/ml. Other details were as specified in the Materials and methods section. ●, Rate of ROS generation; ▲, NAD(P)H level; dashed line, calculated equilibrium NADH level based on the pH-corrected literature equilibrium constant; solid line, theoretical titration curve of the single-electron redox centre with $E_{1/2} = -392$ mV. AcAc, acetoacetate.

results ($K_{eq}^{7.0} = 0.0269$ and $E_{1/2}^{7.0} = -274$ mV, assuming the conventional value of NAD(P)H/NAD(P)$^+$ redox potential of -320 mV) were consistent with the equilibrium constant determined for the free enzyme in Krebs' laboratory [40]. The value of the constant in the literature ($K_{eq}^{7.0} = 0.0493$ [40]) corresponds to a redox potential of -281 mV at pH 7.0. Given the fact that the equilibrium in this system is shifted towards substrates, special precautions were taken to minimize the possible bias of redox titration by endogenous levels of acetoacetate (see the Materials and methods section).

The literature equilibrium constant has been corrected for the difference between the standard pH of 7.0 and the experimental pH of 7.4 (eqn 2):

$$K_{eq}^{pH} = K_{eq}^{7.0} \times 10^{\Delta pH} \quad (2)$$

where ΔpH is the difference between the experimental pH and pH 7.0. The pH-corrected K_{eq} and $E_{1/2}$ were therefore 0.124 and -305 mV respectively.

Next, we performed a redox titration of the rate of H_2O_2 production (Figure 4). Evidently, low concentrations of acetoacetate strongly inhibit rotenone-stimulated ROS production in the presence of β-HOB. To illustrate this point, both the measured NAD(P)H levels and the calculated equilibrium NADH levels based on the pH-corrected literature equilibrium constant (see above) were plotted alongside one another in Figure 4. Similar to the rotenone titration data of Figure 3, the left shift in the plot of ROS production relative to the NADH redox curve is consistent with the existence of a ROS-generating redox centre with a more negative $E_{1/2}$ compared with NADH/NAD$^+$. The solid line on Figure 4 represents the theoretical titration curve of the single-electron redox centre with $E_{1/2} = -392$ mV.

DISCUSSION

The link between cytochrome *c* release and ROS production

Although both cytochrome *c* release and oxidative stress are implicated in various *in vivo* and *in vitro* pathological conditions, less is known about the actual causative link between the two phenomena. In the current study, we show that ROS production is increased in cytochrome *c*-depleted mitochondria oxidizing physiologically relevant NAD$^+$-linked substrates, and that this stimulatory effect can be mimicked with respiratory inhibitors. Inhibition of respiration and stimulation of ROS production observed in cytochrome *c*-depleted mitochondria are reversible upon addition of exogenous cytochrome *c*. The respiratory inhibition leads to reduction of electron carriers upstream of cytochrome *c*, as indicated by NAD(P)H levels. These carriers include both complexes III and I but the similarities with and among the effects of respiratory inhibitors (Tables 1 and 2, and Figure 2) indicate that ROS is generated at a site proximal to the rotenone-binding site. This is consistent with the fact that cytochrome *c* loss inhibits rather than enhances ROS production in complex III (in response to antimycin A) [9].

Because the terminal segment of the respiratory chain has an excess activity over more proximal portions [41–43], one could predict that only substantial cytochrome *c* loss would cause detectable changes in the rate of respiration. The current data suggest that near-complete loss of cytochrome *c* would indeed

enhance ROS production at complex I. Recent publications have reported profound release of cytochrome *c* [44,45] during Fas-, actinomycin D- and staurosporine-activated apoptosis, although the extent of respiratory inhibition resulting specifically from the cytochrome *c* loss is limited [45]. We have observed that Ca^{2+}-induced cytochrome *c* release from brain or neural cell mitochondria is only partial and can lead to mild respiratory inhibition (A. Y. Andreyev, G. Fiskum and A. N. Murphy, unpublished work). Mild respiratory inhibition was observed in cells undergoing apoptosis accompanied by cytochrome *c* release and increased ROS generation [7]. In contrast, the rotenone titration data (Figure 3) show that increased ROS generation requires near-complete respiratory inhibition and NAD(P)$^+$ reduction. Taken together, these data suggest that either partial respiratory inhibition associated with increased ROS results from near-complete cytochrome *c* loss in a subpopulation of mitochondria, or that there may be an indirect link between cytochrome *c* release and ROS production in intact cells undergoing apoptosis.

Comparative studies of heart and brain mitochondria have reported tissue-specific effects on H_2O_2 production [20,30], whereas others did not observe such differences between these tissues [23,46]. In our experiments, brain and heart mitochondria exhibited similar changes in ROS production in response to cytochrome *c* depletion and treatment with respiratory inhibitors, although rates of H_2O_2 production in the presence of inhibitors were higher in brain mitochondria (Table 2).

Mechanism of the ROS production

Mechanisms of ROS production in mitochondria have been a topic of interest over the past decade, but few have concentrated on conditions using NAD^+-linked substrates. Based on the results outlined above as well as on published data, we propose that the rate of ROS production in mitochondria is determined by an ROS-producing redox centre [the site of superoxide generation (*ROS site)] upstream of the rotenone inhibitory site. Similar to the mechanism of ROS production in the ubiquinone-binding site of complex III, the reduced form of this centre (*ROS$^{\bullet-}$) interacts with molecular oxygen irreversibly (eqn 3):

$$*ROS^{\bullet-} + O_2 \rightarrow *ROS + O_2^{\bullet-} \quad (3)$$

with kinetics typical of a bi-molecular mechanism (eqn 4):

$$d[O_2^{\bullet-}]/dt = k[O_2][*ROS^{\bullet-}] \quad (4)$$

where k is the second-order rate constant.

We assume, given the constant oxygen tension, that the reaction actually follows pseudo-first-order kinetics (eqn 5) with the rate simply being proportional to the concentration of the reduced *ROS site:

$$d[O_2^{\bullet-}]/dt = k'[*ROS^{\bullet-}] \quad (5)$$

where k' is the pseudo-first-order rate constant ($k' = k[O_2]$). Therefore, the rate of ROS production can be used as a readout of the redox state of the *ROS site.

Further, we assume that the redox status of the *ROS site is under thermodynamic control of the NADH/NAD^+ couple (eqn 6). In this case, the reduction of the *ROS site is regulated by the NADH/NAD^+ ratio rather than the NADH level (eqns 7 and 8), consistent with a non-linear dependence of ROS production on the NAD(P)H level. Indeed, a large increase in NAD(P)H level from zero to approx. 85% of maximal has a very slight effect on ROS production, whereas small changes above the 85% level correspond to profound stimulation of ROS generation (Figures 3 and 4). Note that these small changes in NADH correspond to large changes in NAD^+, the denominator in eqn (8), and therefore large changes in the NADH/NAD^+ ratio. These results are inconsistent with the alternative model of simple kinetic control in which the rate of the reaction is always proportional to the level of substrate (i.e. NADH). In the kinetic control models, the regulation by the NADH/NAD^+ ratio could potentially arise from NAD^+ competing with NADH for a binding site but, given the low apparent affinity of NAD^+ for complex I [47], this scenario seems unlikely.

$$NADH + (2/n)*ROS \leftrightarrow NAD^+ + (2/n)*ROS^{\bullet n-} + H^+ \quad (6)$$

where n is number of electrons accepted by the *ROS site and

$$K_{eq} = [NAD^+][*ROS^{\bullet n-}]^{(2/n)}/[NADH][*ROS]^{(2/n)} \quad (7)$$

Therefore

$$([*ROS^{\bullet n-}]/[*ROS])^{(2/n)} = K_{eq}([NADH]/[NAD^+]) \quad (8)$$

where $K_{eq} < 1$.

The assumption of the thermodynamic control of the *ROS site is also internally consistent given the fact that the rate of ROS production (below 300 pmol/min per mg of protein in heart mitochondria; see Table 2) is very low compared with the rate of electron transport in the respiratory chain (around 100 nmol/min per mg of protein; e.g. see Figure 1).

The requirement of a highly reduced state of NAD^+ to support ROS production indicates that reduction of the *ROS centre (eqn 6) is thermodynamically unfavourable, i.e. the equilibrium is shifted to the left ($K_{eq} < 1$) and $E_{1/2}$ of the *ROS site is more negative than NADH/NAD^+. To estimate the $E_{1/2}$ value using the redox titration approach, β-HOB oxidation (eqn 1) was employed to generate NADH for eqn (6) resulting in the overall eqn (9):

$$\beta\text{-HOB} + (2/n)*ROS \leftrightarrow \text{acetoacetate} + (2/n)*ROS^{\bullet n-} + 2H^+ \quad (9)$$

Regression analysis of the redox titration data (Figure 4) indicates that the *ROS site behaves as a single-electron redox centre (apparent $n = 1.18$) with an apparent standard potential, $E_{1/2}^{7.4}$, of -392 mV at our experimental pH of 7.4.

It is tempting to speculate, based on these redox properties, that the prime candidate for the *ROS site is the N-1a Fe–S centre in complex I ($E_{1/2}^{7.2} = -380 \pm 20$ mV, e.g. [48,49]). Although the role of this centre in electron transport and its ability to be reduced by NADH remains debatable, this is the only component of the respiratory chain with a redox potential substantially more negative than the NADH/NAD^+ couple. Redox titration of the *ROS site in intact mitochondria reported here is in fairly good agreement with the published results on more direct measurements of superoxide formation in submitochondrial particles using the NADH/NAD^+ redox couple [50]. In their data, the half-maximal superoxide production required a NADH/NAD^+ ratio of approx. 3, consistent with the concept of a more negative $E_{1/2}$ for the ROS-generating site compared with NADH. They observed a pH-dependent shift of the redox titration curve between pH 6.8 and 7.6, consistent with one proton being consumed rather than released in eqn (6), as would happen if the *ROS centre was protonated. If this is the case, eqn (6) converts into the form of eqn (10), consistent with reports in the literature that the N-1a Fe–S centre is capable of being protonated [51].

$$NADH + 2*ROS + H^+ \leftrightarrow NAD^+ + 2*ROSH^{\bullet} \quad (10)$$

In this case, the standard potential of the *ROS site must be less negative at pH 7.0, becoming $E_{1/2}^{7.0} = -369$ mV. One may speculate that, although mechanistically unnecessary, the highly negative redox potential of the N-1a centre evolved from a natural selection process to minimize ROS generation.

The alternative is that mitochondrial ROS generation in the presence of physiological substrates occurs outside of the res-

piratory chain. For instance, Krishnamoorthy and Hinkle [50] discuss lipoamide dehydrogenase as an 'attractive possibility', but rule it out based on low abundance of the enzyme in their preparation of submitochondrial particles. Presumption of complex I as being the source of mitochondrial ROS originated from the experiments with submitochondrial preparations (e.g. [15,50]) or isolated complex I [31,52], where the possible interference from non-respiratory chain components is much less likely. A recent publication [23], which demonstrates inhibition of rotenone-induced ROS production by diphenyleneiodonium ('DPI'), a flavin-modifying agent with certain specificity towards FMN of complex I, suggests that the *ROS site in intact mitochondria is located at or downstream of a flavin. ROS production in the site proximal to the rotenone-binding site is completely inhibited by *p*-chloromercuriobenzoate [36], a thiol reagent that blocks Fe–S clusters of complex I. Although the latter two results are in agreement with the concept of the Fe–S centre N-1a of complex I being the *ROS site, the low selectivity of both diphenyleneiodonium and *p*-chloromercuriobenzoate does not allow unequivocal identification of the site. The redox properties described above exclude reduced FMN itself as the *ROS site. If future studies favour the alternative location of the *ROS site, we would anticipate it to be a highly negative single-electron acceptor, probably an Fe–S cluster, linked to a flavin.

The understanding of the mechanism of ROS generation allows the potential design of novel therapeutic strategies to relieve oxidative stress. Conventional wisdom might dictate a beneficial effect of achieving the maximally reduced state of mitochondrial matrix components based on the requirement of reducing equivalents for the glutathione-dependent antioxidant system. This approach may need reassessment given the steep rise of ROS production at highly reduced states of mitochondrial $NAD(P)^+$. Instead, it may be advantageous to aim at achieving a slightly oxidized (approx. 85% reduced) state of $NAD(P)^+$ at which the ROS production virtually ceases while the reducing power is preserved to reduce glutathione. This strategy is complementary to the one proposed by Skulachev [53], in which mild uncoupling serves to decrease the local concentration of free oxygen. The general approach in both cases would be essentially the same, i.e. to promote uncoupled and/or non-coupled respiration [54]. This concept is in keeping with an inherent protective mechanism of superoxide-induced stimulation of uncoupling protein activity that was recently proposed [55]. The particular choice of strategy is dependent upon the nature of the initial damage causing oxidative stress. In the case of a respiratory chain defect (e.g. profound cytochrome release), the tool of choice would be an electron-shuttling compound allowing bypass of the damaged site. Alternatively, if the initial damage leads to transition of mitochondria to metabolic State 4 (e.g. decreased supply of substrates for the ATP synthase or decreased energy utilization), 'mild uncoupling' [53,56] would be a strategy of choice.

We thank Dr Andrei Vinogradov and Dr Neil Howell for critical reading of the manuscript, Dr James Dykens and Dr Anatoly Starkov for helpful discussion and Adam Prince for technical assistance.

REFERENCES

1 Murphy, A. N., Fiskum, G. and Beal, M. F. (1999) Mitochondria in neurodegeneration: bioenergetic function in cell life and death. J. Cereb. Blood Flow Metab. **19**, 231–245

2 Cai, J. and Jones, D. P. (1999) Mitochondrial redox signaling during apoptosis. J. Bioenerg. Biomembr. **31**, 327–334

3 Raha, S. and Robinson, B. H. (2001) Mitochondria, oxygen free radicals, and apoptosis. Am. J. Med. Genet. **106**, 62–70

4 Skulachev, V. P. (1998) Cytochrome c in the apoptotic and antioxidant cascades. FEBS Lett. **423**, 275–280

5 Atlante, A., Calissano, P., Bobba, A., Azzariti, A., Marra, E. and Passarella, S. (2000) Cytochrome c is released from mitochondria in a reactive oxygen species (ROS)-dependent fashion and can operate as a ROS scavenger and as a respiratory substrate in cerebellar neurons undergoing excitotoxic death. J. Biol. Chem. **275**, 37159–37166

6 Jacobs, E. E. and Sanadi, D. R. (1960) Phosphorylation couples to electron transport mediated by high potential electron carriers. Biochim. Biophys. Acta **38**, 12–33

7 Cai, J. and Jones, D. P. (1998) Superoxide in apoptosis. Mitochondrial generation triggered by cytochrome c loss. J. Biol. Chem. **273**, 11401–11404

8 Krohn, A. J., Wahlbrink, T. and Prehn, J. H. M. (1999) Mitochondrial depolarization is not required for neuronal apoptosis. J. Neurosci. **19**, 7394–7404

9 Turrens, J. F., Alexandre, A. and Lehninger, A. L. (1985) Ubisemiquinone is the electron donor for superoxide formation by complex III of heart mitochondria. Arch. Biochem. Biophys. **237**, 408–414

10 Boveris, A. and Chance, B. (1973) The mitochondrial generation of hydrogen peroxide. General properties and effect of hyperbaric oxygen. Biochem. J. **134**, 707–716

11 Boveris, A., Cadenas, E. and Stoppani, A. O. M. (1976) Role of ubiquinone in the mitochondrial generation of hydrogen peroxide. Biochem. J. **156**, 435–444

12 Ksenzenko, M., Konstantinov, A. A., Khomutov, G. B., Tikhonov, A. N. and Ruuge, E. K. (1983) Effect of electron transfer inhibitors on superoxide generation in the cytochrome bc1 site of the mitochondrial respiratory chain. FEBS Lett. **155**, 19–24

13 Trumpower, B. L. (1990) The protonmotive Q cycle. Energy transduction by coupling of proton translocation to electron transfer by the cytochrome bc_1 complex. J. Biol. Chem. **265**, 11409–11412

14 Cadenas, E., Boveris, A., Ragan, C. I. and Stoppani, A. O. (1977) Production of superoxide radicals and hydrogen peroxide by NADH-ubiquinone reductase and ubiquinol-cytochrome c reductase from beef-heart mitochondria. Arch. Biochem. Biophys. **180**, 248–257

15 Turrens, J. F. and Boveris, A. (1980) Generation of superoxide anion by the NADH dehydrogenase of bovine heart mitochondria. Biochem. J. **191**, 421–427

16 Cino, M. and Del Maestro, R. F. (1989) Generation of hydrogen peroxide by brain mitochondria: the effect of reoxygenation following postdecapitative ischemia. Arch. Biochem. Biophys. **269**, 623–638

17 Hansford, R. G., Hogue, B. A. and Mildaziene, V. (1997) Dependence of H_2O_2 formation by rat heart mitochondria on substrate availability and donor age. J. Bioenerg. Biomembr. **29**, 89–95

18 Korshunov, S. S., Skulachev, V. P. and Starkov, A. A. (1997) High protonic potential actuates a mechanism of production of reactive oxygen species in mitochondria. FEBS Lett. **416**, 15–18

19 Korshunov, S. S., Korkina, O. V., Ruuge, E. K., Skulachev, V. P. and Starkov, A. A. (1998) Fatty acids as natural uncouplers preventing generation of $O_2^{\bullet -}$ and H_2O_2 by mitochondria in the resting state. FEBS Lett. **435**, 215–218

20 Kwong, L. K. and Sohal, R. S. (1998) Substrate and site specificity of hydrogen peroxide generation in mouse mitochondria. Arch. Biochem. Biophys. **350**, 118–126

21 Hinkle, P., Butow, R. A., Racker, E. and Chance, B. (1967) Partial resolution of the enzymes catalyzing oxidative phosphorylation. XV. Reverse electron transfer in the flavin-cytochrome beta region of the respiratory chain of beef heart submitochondrial particles. J. Biol. Chem. **242**, 5169–5173

22 Chance, B., Sies, H. and Boveris, A. (1979) Hydroperoxide metabolism in mammalian organs. Physiol. Rev. **59**, 527–605

23 Liu, Y., Fiskum, G. and Schubert, D. (2002) Generation of reactive oxygen species by the mitochondrial electron transport chain. J. Neurochem. **80**, 780–787

24 Kushnareva, Y., Andreyev, A. and Murphy, A. N. (2001) Reactive oxygen species generation by mitochondria in pathophysiological models. Biophys. J. **80**, 45a

25 Rosenthal, R. E., Hamud, F., Fiskum, G., Varghese, P. J. and Sharpe, S. (1987) Cerebral ischemia and reperfusion: prevention of brain mitochondrial injury by lidoflazine. J. Cereb. Blood Flow Metab. **7**, 752–758

26 Andreyev, A. and Fiskum, G. (1999) Calcium induced release of mitochondrial cytochrome c by different mechanisms selective for brain versus liver. Cell Death Differ. **6**, 825–832

27 Sokolove, P. M. and Shinaberry, R. G. (1988) Na^+-independent release of Ca^{2+} from rat heart mitochondria. Induction by adriamycin aglycone. Biochem. Pharmacol. **37**, 803–812

28 Loschen, G., Flohe, L. and Chance, B. (1971) Respiratory chain linked H_2O_2 production in pigeon heart mitochondria. FEBS Lett. **18**, 261–264

29 Liu, S. S. (1997) Generating, partitioning, targeting and functioning of superoxide in mitochondria. Biosci. Rep. **17**, 259–272

30 Herrero, A. and Barja, G. (1997) ADP-regulation of mitochondrial free radical production is different with complex I- or complex II-linked substrates: implications for the exercise paradox and brain hypermetabolism. J. Bioenerg. Biomembr. **29**, 241–249

31 Takeshige, K., Takayanagi, R. and Minakami, S. (1980) Lipid peroxidation and the reduction of ADP-Fe^{3+} chelate by NADH-ubiquinone reductase preparation from bovine heart mitochondria. Biochem. J. **192**, 861–866

32 Barja, G. and Herrero, A. (1998) Localization at complex I and mechanism of the higher free radical production of brain nonsynaptic mitochondria in the short-lived rat than in the longevous pigeon. J. Bioenerg. Biomembr. **30**, 235–243

33 Fabre, E., Monserrat, J., Herrero, A., Barja, G. and Leret, M. L. (1999) Effect of MPTP on brain mitochondrial H_2O_2 and ATP production and on dopamine and DOPAC in the striatum. J. Physiol. Biochem. **55**, 325–331

34 Hensley, K., Pye, Q. N., Maidt, M. L., Stewart, C. A., Robinson, K. A., Jaffrey, F. and Floyd, R. A. (1998) Interaction of α-phenyl-N-tert-butyl nitrone and alternative electron acceptors with complex I indicates a substrate reduction site upstream from the rotenone binding site. J. Neurochem. **71**, 2549–2557

35 Lenaz, G. (2001) The mitochondrial production of reactive oxygen species: mechanisms and implications in human pathology. IUBMB Life **52**, 159–164

36 Genova, M. L., Ventura, B., Giuliano, G., Bovina, C., Formiggini, G., Parenti Castelli, G. and Lenaz, G. (2001) The site of production of superoxide radical in mitochondrial complex I is not a bound ubisemiquinone but presumably iron-sulfur cluster N2. FEBS Lett. **505**, 364–368

37 Betarbet, R., Sherer, T. B., MacKenzie, G., Garcia-Osuna, M., Panov, A. V. and Greenamyre, J. T. (2000) Chronic systemic pesticide exposure reproduces features of Parkinson's disease. Nat. Neurosci. **3**, 1301–1306

38 Ramsay, R. R. and Singer, T. P. (1992) Relation of superoxide generation and lipid peroxidation to the inhibition of NADH-Q oxidoreductase by rotenone, piericidin A, and MPP^+. Biochem. Biophys. Res. Commun. **189**, 47–52

39 Votyakova, T. V. and Reynolds, I. J. (2001) $\Delta\Psi_m$-dependent and -independent production of reactive oxygen species by rat brain mitochondria. J. Neurochem. **79**, 266–277

40 Williamson, D. H., Lund, P. and Krebs, H. A. (1967) The redox state of free nicotinamide-adenine dinucleotide in the cytoplasm and mitochondria of rat liver. Biochem. J. **103**, 514–527

41 Davey, G. P., Peuchen, S. and Clark, J. B. (1998) Energy thresholds in brain mitochondria. Potential involvement in neurodegeneration. J. Biol. Chem. **273**, 12753–12757

42 Gnaiger, E., Lassnig, B., Kuznetsov, A., Rieger, G. and Margreiter, R. (1998) Mitochondrial oxygen affinity, respiratory flux control and excess capacity of cytochrome c oxidase. J. Exp. Biol. **201**, 1129–1139

43 Rossingnol, R., Letellier, T., Malgat, M., Rocher, C. and Mazat, J. P. (2000) Tissue variation in the control of oxidative phosphorylation: implication for mitochondrial diseases. Biochem. J. **347**, 45–53

44 Goldstein, J. C., Waterhouse, N. J., Juin, P., Evan, G. I. and Green, D. R. (2000) The coordinate release of cytochrome c during apoptosis is rapid, complete and kinetically invariant. Nat. Cell Biol. **2**, 156–162

45 Mootha, V. K., Wei, M. C., Buttle, K. F., Scorrano, L., Panoutsakopoulou, V., Mannella, C. and Korsmeyer, S. J. (2001) A reversible component of mitochondrial respiratory dysfunction in apoptosis can be rescued by exogenous cytochrome c. EMBO J. **20**, 661–671

46 Starkov, A. A. and Fiskum, G. (2001) Myxothiazol induces H_2O_2 production from mitochondrial respiratory chain. Biochem. Biophys. Res. Commun. **281**, 645–650

47 Vinogradov, A. D. and Grivennikova, V. G. (2001) The mitochondrial complex I: progress in understanding of catalytic properties. IUBMB Life **52**, 129–134

48 Ohnishi, T. (1975) Thermodynamic and EPR characterizaton of iron-sulfur centers in the NADH-ubiquinone segment of the mitochondrial repiratory chain in pigeon heart. Biochim. Biophys. Acta **387**, 475–490

49 Ohnishi, T. (1976) Studies on the mechanism of site I energy conservation. Eur. J. Biochem. **64**, 91–103

50 Krishnamoorthy, G. and Hinkle, P. (1988) Studies on the electron transfer pathway, topography of iron-sulfur centers, and site of coupling in NADH-Q oxidoreductase. J. Biol. Chem. **263**, 17566–17575

51 Ingledew, W. J. and Ohnishi, T. (1980) An analysis of some thermodynamic properties of iron-sulphur centers in site I of mitochondria. Biochem. J. **186**, 111–117

52 Kang, D., Narabayashi, H., Sata, T. and Takeshige, K. (1983) Kinetics of superoxide formation by respiratory chain NADH-dehydrogenase of bovine heart mitochondria. J. Biochem. (Tokyo) **94**, 1301–1306

53 Skulachev, V. P. (1996) Role of uncoupled and non-coupled oxidations in maintenance of safely low levels of oxygen and its one-electron reductants. Q. Rev. Biophys. **29**, 169–202

54 Skulachev, V. P. (1998) Uncoupling: new approaches to an old problem of bioenergetics. Biochim. Biophys. Acta **1363**, 100–124

55 Echtay, K. S., Roussel, D., St-Pierre, J., Jekabsons, M. B., Cadenas, S., Stuart, J. A., Harper, J. A., Roebuck, S. J., Morrison, A., Pickering, S., Clapham, J. C. and Brand, M. D. (2002) Superoxide activates mitochondrial uncoupling proteins. Nature (London) **415**, 96–99

56 Starkov, A. A. (1997) 'Mild' uncoupling of mitochondria. Biosci. Rep. **17**, 273–279

Received 16 July 2002; accepted 15 August 2002
Published as BJ Immediate Publication 15 August 2002, DOI 10.1042/BJ20021121